electronic reprint

Journal of
Applied Crystallography
ISSN 0021-8898

New five-circle κdiffractometer for reference-beam diffraction studies

Daniel Pringle and Qun Shen

Journal of
Applied Crystallography
ISSN 0021-8898

Received 18 June 2002
Accepted 27 September 2002

New five-circle κ diffractometer for reference-beam diffraction studies

Daniel Pringle and Qun Shen*

Cornell High Energy Synchrotron Source, Wilson Laboratory, Cornell University, Ithaca, NY 14853, USA. Correspondence e-mail: qs11@cornell.edu

A compact five-circle κ-geometry diffractometer has been designed and implemented at CHESS for automated reference-beam X-ray diffraction (RBD) experiments. The details of the diffractometer design are presented, along with its geometry calculations, and its alignment and control algorithm. An outline of the overall RBD experimental procedure has been developed based on this κ diffractometer. Measured RBD interference profiles from a lysozyme crystal demonstrate that efficient triplet-phase data collection is possible using this new device in a modified crystallography oscillation setup.

1. Introduction

It has been demonstrated recently (Shen, 1998, 1999*a*; Chang *et al.*, 1999; Shen *et al.*, 2000*a*,*b*; Shen & Huang, 2001; Chao *et al.*, 2002) that reference-beam diffraction (RBD) or multi-beam imaging, a technique that incorporates the principle of three-beam diffraction (Colella, 1974; Chang, 1982; Weckert & Hummer, 1997) into the popular oscillating-crystal data collection method in protein crystallography, can be a practical and efficient way to measure a large number of phase-sensitive three-beam interference profiles using an area detector. The technique requires an excitation of a strong Bragg reflection **G** in such a way that its reciprocal-space vector **G** is brought parallel to the oscillation axis ψ, which is then tilted to the Bragg angle θ_G with respect to the incident X-ray beam. In general, existing crystallographic oscillation camera setups, including those equipped with a standard κ diffractometer, do not provide this capability because of the limited number of rotational degrees of freedom.

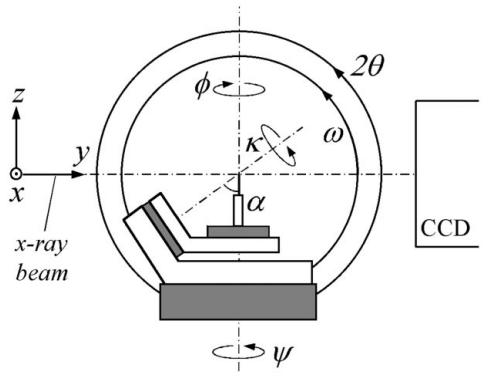

Figure 1
Schematic design of the five-circle κ diffractometer, with four rotation controls for the sample, ω, ψ, κ, φ, plus a 2θ rotation for a pin-diode detector (not shown). The κ angle is chosen to be $\alpha = 50^\circ$. The geometry shown corresponds to the default diffractometer zero position at $\psi = 0$, with the φ axis parallel to ψ and the κ stage at its most upstream position with respect to the incident X-ray beam. Also shown is an X-ray CCD camera that is fixed in space and is used to record phase-sensitive reference-beam diffraction images.

At the Cornell High Energy Synchrotron Source (CHESS) we have designed and implemented a novel compact five-circle κ diffractometer to perform the necessary tasks for reference-beam diffraction experiments. As shown in Fig. 1, the key feature in the new instrument, as compared with a standard κ diffractometer, is an oscillation axis ψ inserted between the κ and the ω axes to provide the required extra degree of freedom. In this paper, we present the basic geometry and a detailed control algorithm of the five-circle κ diffractometer, and provide some initial test results on a protein crystal using the diffractometer in an RBD experiment.

2. Diffractometer design

In order to bring an arbitrary Bragg reflection **G** into its diffraction condition in the vertical plane, a standard approach is to use three rotations (φ, χ, ω) as in an Eulerian four-circle geometry (Busing & Levy, 1967). It is possible in this approach to realise a rotation around the scattering vector **G**, usually called the azimuthal rotation ψ, by a combination of (φ, χ, ω) angular settings. However, if this method is adopted for reference-beam diffraction experiments, it would require movements of three motors (φ, χ, ω) simultaneously for any oscillation range $\Delta\psi$, which lacks the required mechanical precision due to finite motor steps and is difficult to implement in any crystallographic software packages for oscillation camera controls.

Two advanced six-circle diffractometers have been developed for the purpose of precise control of the azimuthal angle ψ in three-beam diffraction experiments (Weckert & Hummer, 1997; Thorkildsen *et al.*, 1999). These designs could be adapted for reference-beam measurements, but the large size and the high cost of these ψ-circle diffractometers would be problematic for their incorporation into a standard oscil-

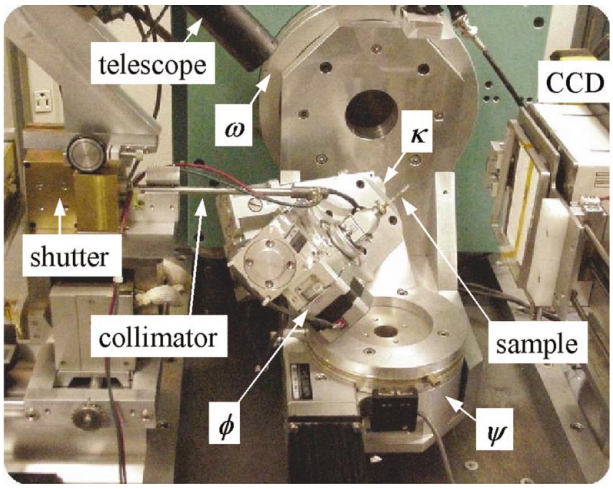

Figure 2
Picture of the new κ diffractometer used in a reference-beam diffraction experiment.

lation camera for crystallography, where a compact device is preferred.

As shown in Fig. 1, the new five-circle κ diffractometer that we have designed is built on top of a compact ω–2θ two-circle goniometer (Huber 424; Huber, 2001). A Huber 410 rotation stage is mounted on the ω stage and serves as the oscillation axis ψ, orthogonal to the ω axis. On top of the ψ circle, a small two-circle (κ, φ) goniometer, consisting of two Huber 408 devices, is constructed in a 50° κ geometry and is used to bring any given Bragg reflection **G** parallel to the ψ axis. A standard goniometer head with a height of 49 mm can be used on the φ axis for sample mounting, and a small pin-diode is mounted on the 2θ arm for measurements of the reference **G** reflection rocking curves for alignment purposes.

The complete κ diffractometer has been designed, assembled and tested in-house at CHESS. Fig. 2 shows a picture of the diffractometer in an actual RBD experiment. All rotations on the diffractometer are controlled by stepping motors, except the oscillation axis ψ which is controlled by a DC servo motor in order to minimize vibrations induced by a stepping motor. The intrinsic alignment of the multiple axes on the diffractometer is achieved by iteratively adjusting the mounting adapter plate positions between the rotation stages. Using a sharp centering pin and a high-power magnifying telescope, a very low sphere of confusion of 30 µm peak-to-peak has been achieved for the three inner circles (φ, κ, ψ), and about 50 µm peak-to-peak is achievable if the ω axis is included. The angles between the different rotation axes are determined by precisely machined adapter plates and have been checked with a properly placed machinist level to within 30 arcsec of the respective design values. Such precision is quite adequate for reference-beam experiments on protein single crystals.

3. Geometry calculations

The (φ, κ, ω, 2θ) rotations on the diffractometer are controlled by *SPEC* software (Certified Scientific Software, 2002) on a Unix computer, while the ψ axis is controlled by oscillation software provided by Area Detector Systems Corporation (ADSC, 2001). When a fresh sample crystal is mounted, an initial oscillation diffraction image is taken at the default position of the κ diffractometer, as shown in Fig. 1, where all sample rotation angles are defined as zero: $\varphi = \kappa = \omega = \psi = 0$. This diffraction image is indexed by a crystallographic analysis program, *MOSFLM* (Collaborative Computational Project, Number 4, 1994), from which the initial orientation matrix **U** of the crystal with respect to the diffractometer is obtained. We then choose a particular Bragg reflection **G** = (h, k, l) as the reference reflection, the coordinates of which, in the (x, y, z) system shown in Fig. 1, are given by the orientation matrix **U**:

$$\begin{pmatrix} G_x \\ G_y \\ G_z \end{pmatrix} = \mathbf{U} \begin{pmatrix} h \\ k \\ l \end{pmatrix}. \qquad (1)$$

The next step is to calculate the necessary angular settings of (φ, κ) to bring **G** parallel to the ψ axis in the $+z$ direction.

To do this we have adapted the general analytical approach of Thorkildsen *et al.* (1999), in which an intuitive conic-section method is used to understand the very general operation of a six-circle κ diffractometer. Our geometry has only five circles as we have only one detector degree of freedom, but aside from this and a different choice of coordinate system, the two geometries are analogous and Thorkildsen's method can be applied straightforwardly to our case.

The essence of the conic-section approach is that a sequence of consecutive rotations (φ, κ, ψ, ω) of a reciprocal-space vector **G** can be described by the individual conic sections swept out by the vector under each rotation. Once we define a zero point for each rotation, we can envisage the **G**

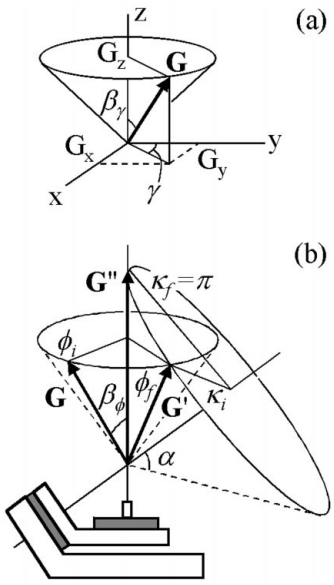

Figure 3
(*a*) Inclination (β_γ) and rotation (γ) angles for parameterization of the position of **G** along a rotational conic section. (*b*) Conic sections of φ and κ rotations for the new κ diffractometer, showing the initial and final values of each angle.

vector being swept along one such cone from some initial position to a final position. These cones are parameterized by the angle of inclination from the cone axis, β_γ, and the rotation angle γ, as shown in Fig. 3(*a*). Each rotation sweeps **G** from an initial position defined by β_γ and γ_i to a final position β_γ and γ_f, which then defines the starting position for the next rotation around another axis, and so on.

In our case, as shown in Fig. 3(*b*), we first rotate **G** into **G**′ by a φ rotation around the $+z$ axis, and then **G**′ into **G**″ by a κ rotation around the κ axis which is inclined by angle α from the $+z$ axis. Both rotations are assumed to be left-handed for positive values of φ and κ. In the φ rotation, the coordinates **G** = (G_x, G_y, G_z) transform according to the following rule:

$$\begin{pmatrix} G_x \\ G_y \\ G_z \end{pmatrix}_\varphi = G \begin{pmatrix} \sin\beta_\varphi \sin\varphi \\ \sin\beta_\varphi \cos\varphi \\ \cos\beta_\varphi \end{pmatrix}, \tag{2}$$

with $G = |\mathbf{G}|$, while in the κ rotation, the expression becomes somewhat more complex since it involves an additional rotation α of the cone axis around the $+x$ direction:

$$\begin{aligned} \begin{pmatrix} G_x \\ G_y \\ G_z \end{pmatrix}_\kappa &= G\,\mathbf{R}_x(\alpha) \begin{pmatrix} \sin\beta_\kappa \sin\kappa \\ \sin\beta_\kappa \cos\kappa \\ \cos\beta_\kappa \end{pmatrix} \\ &= G \begin{pmatrix} \sin\beta_\kappa \sin\kappa \\ \cos\alpha \sin\beta_\kappa \cos\kappa + \sin\alpha \cos\beta_\kappa \\ -\sin\alpha \sin\beta_\kappa \cos\kappa + \cos\alpha \cos\beta_\kappa \end{pmatrix}. \end{aligned} \tag{3}$$

The initial orientation angles, β_φ and φ_i, of **G** are determined by the (G_x, G_y, G_z) components from the initial orientation matrix **U**:

$$\sin\varphi_i = \frac{G_x}{(G_x^2 + G_y^2)^{1/2}}, \qquad \cos\varphi_i = \frac{G_y}{(G_x^2 + G_y^2)^{1/2}}, \tag{4}$$

and

$$\sin\beta_\varphi = \frac{(G_x^2 + G_y^2)^{1/2}}{G}, \qquad \cos\beta_\varphi = \frac{G_z}{G}. \tag{5}$$

The final position **G**″ is along the $+z$ axis, which has an inclination angle $\beta_\kappa = \alpha$ with respect to the κ axis. From equation (3), we obtain the following equation for the final position of **G**:

$$\begin{pmatrix} G_x'' \\ G_y'' \\ G_z'' \end{pmatrix} = \begin{pmatrix} 0 \\ 0 \\ G \end{pmatrix} = G \begin{pmatrix} \sin\alpha \sin\kappa_f \\ \cos\alpha \sin\alpha \cos\kappa_f + \sin\alpha \cos\alpha \\ -\sin\alpha \sin\alpha \cos\kappa_f + \cos\alpha \cos\alpha \end{pmatrix},$$

which has a unique solution for non-zero α:

$$\kappa_f = \pi. \tag{6}$$

The intermediate position **G**′ can be reached either from the initial position **G** by a φ rotation from φ_i to φ_f, or from the final position **G**″ by a κ rotation from κ_f to κ_i. Equating (2) for φ_f to (3) for κ_i, we have

$$\begin{pmatrix} \sin\beta_\varphi \sin\varphi_f \\ \sin\beta_\varphi \cos\varphi_f \\ \cos\beta_\varphi \end{pmatrix} = \begin{pmatrix} \sin\beta_\kappa \sin\kappa_i \\ \cos\alpha \sin\beta_\kappa \cos\kappa_i + \sin\alpha \cos\beta_\kappa \\ -\sin\alpha \sin\beta_\kappa \cos\kappa_i + \cos\alpha \cos\beta_\kappa \end{pmatrix}.$$

Inserting $\beta_\kappa = \alpha$ yields

$$\begin{pmatrix} \sin\beta_\varphi \sin\varphi_f \\ \sin\beta_\varphi \cos\varphi_f \\ \cos\beta_\varphi \end{pmatrix} = \begin{pmatrix} \sin\alpha \sin\kappa_i \\ \cos\alpha \sin\alpha(1 + \cos\kappa_i) \\ \cos^2\alpha - \sin^2\alpha \cos\kappa_i \end{pmatrix}. \tag{7}$$

Equation (7) provides two independent equations for two unknowns, φ_f and κ_i. The solutions are given by

$$\cos\varphi_f = \frac{\cos\alpha(1 - \cos\beta_\varphi)}{\sin\alpha \sin\beta_\varphi}, \qquad \cos\kappa_i = \frac{\cos^2\alpha - \cos\beta_\varphi}{\sin^2\alpha}. \tag{8}$$

We note that the sines for φ_f and κ_i are not uniquely determined. However, their signs are constrained by

$$\sin\kappa_i = \frac{\sin\beta_\varphi}{\sin\alpha} \sin\varphi_f, \tag{9}$$

which yields two possible solutions, corresponding to an arbitrary choice of the sign for $\sin\kappa_i$ or for $\sin\varphi_f$.

From equations (1), (4), (5) and (8), the final rotations φ and κ that bring **G** along the z axis, the so-called aligning rotations, are given by the difference in their corresponding final and initial values:

$$\varphi = \varphi_f - \varphi_i, \qquad \kappa = \kappa_f - \kappa_i. \tag{10}$$

Because of the sign ambiguity discussed above, there are two sets of aligning angles $\{\varphi, \kappa\}$ corresponding to $\pm\kappa_i$, and either will align **G** parallel to the $+z$ axis. This is due to the fact that in general the φ and the κ cones have two intersecting lines, as can be seen clearly in Fig. 3(*b*).

It is obvious from Fig. 3(*b*) that the intersection of the two cones is only possible when $\beta_\varphi < 2\alpha$, which is 100° for our diffractometer. Thus it would not be possible to use the diffractometer to align a reflection physically if its initial inclination angle β_φ with respect to $+z$ were larger than 2α. In addition, in order to avoid obstruction of the incident X-ray beam, we also restrict κ to $|\kappa| < 120°$. In practice these constraints can be alleviated by choosing one of several symmetry-equivalent reflections of the original **G** that needs to be aligned.

After applying the aligning rotations (φ, κ), the reference **G** reflection is brought into its Bragg condition with an $\omega = \theta_G$ rotation, where θ_G is the Bragg angle for **G**. For precise alignment of low-mosaic-spread crystals, each of the $(\varphi, \kappa, \omega)$ axes is equipped with a gear-reducer to provide better than 0.0005° resolution in angular movements. Finally, a $2\theta = 2\theta_G$ rotation is used to bring the 2θ arm into its position to check the **G** reflection rocking curve with the pin-diode detector.

4. Experimental procedure

We have conducted several reference-beam diffraction experiments at CHESS on tetragonal lysozyme crystals using the new κ diffractomter and the geometry calculations described in the previous section. Based on these test runs, an

experimental procedure for reference-beam diffraction measurements has been established, as illustrated in Fig. 4.

Starting from a fresh sample crystal, we first record an oscillation diffraction pattern in the default diffractometer position, as shown Fig. 1(*a*). This image is processed with the *MOSFLM* software package to refine the crystal cell and generate the orientation matrix **U**. We next apply the aligning rotations $\{\varphi, \kappa\}$ as determined by equation (9) to bring a chosen reference reflection **G** onto the oscillation axis $\psi = +z$. The ψ axis is then tilted by an ω rotation of Bragg angle θ_G to bring **G** into its diffraction condition.

To check the alignment of **G**, we measure the **G** rocking curves at four ψ positions: $\psi = 0, 180^\circ, \psi_0$ and $\psi_0 + 180^\circ$, with ψ_0 as close to 90° as possible. We have found that the peak positions in these four rocking curves generally agree with each other to within about 0.5°, which is acceptable but not good enough for high-quality protein crystals with extremely narrow mosaicity. The origins for this alignment error may lie in the intrinsic indexing accuracy of *MOSFLM*, or in a slight deviation from the default diffractometer zero position when the initial oscillation image is taken.

This misalignment error can be corrected by the following realignment procedure. First, we calculate the components of the azimuthal inclination of **G** from the four ω peak positions in the rocking-curve measurements along the two directions $\psi = 0$ and $\psi = \psi_0$. This leads to a set of (G''_x, G''_y, G''_z) components for the misaligned final position $\mathbf{G}''$. We then apply the inverse of the previously performed aligning rotations $\{\varphi, \kappa\}$ to (G''_x, G''_y, G''_z) to arrive at a revised initial position (G_x, G_y, G_z) of **G**. The new (G_x, G_y, G_z) coordinates represent the corrected initial position that **G** should have been in to have ended up in the misaligned position under the applied rotations. A revised set of alignment angles $\{\varphi', \kappa'\}$ are then calculated from the new (G_x, G_y, G_z) coordinates using the same routine described in the previous section, and the differences $\Delta\varphi = \varphi' - \varphi$ and $\Delta\kappa = \kappa' - \kappa$ in the recalculated and original angles are applied as corrections to the original $\{\varphi, \kappa\}$. We have found that this realigning procedure works very well and can often reduce misalignment from ~0.5° to better than 0.01° by only one such iteration.

With reference reflection **G** aligned parallel to the oscillation axis ψ, reference-beam data collection can proceed in a way that closely follows the standard oscillating-crystal method. A slight modification to the oscillation control has been implemented so that phase-sensitive RBD oscillation images can be recorded on a charge-coupled device (CCD) by multiple exposures at several (typically 10 to 20) $\omega = \omega_i$ steps through the **G** reflection rocking curve. The rocking curve is measured in the increasing-ω direction, corresponding to the **G** reciprocal node moving from outside to inside the Ewald sphere. Typical exposure time for each oscillation image is 15–30 s for lysozyme crystals at CHESS bent-magnet stations. The RBD oscillation images are then indexed, and integrated intensities $I_H(\omega_i)$ for each recorded Bragg peak **H** are obtained using standard crystallography software packages, such as *MOSFLM*.

The intensity profile $I_H(\omega_i)$ typically exhibits an interference effect, as shown in Fig. 5, that contains the triplet-

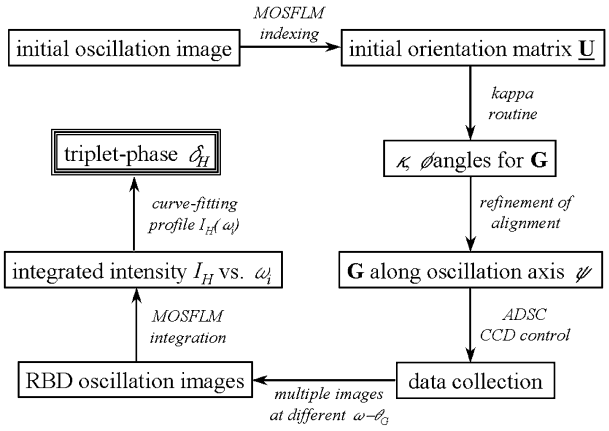

Figure 4
Experimental procedure for reference-beam diffraction measurements of triplet phases on a protein crystal, using the five-circle κ diffractometer.

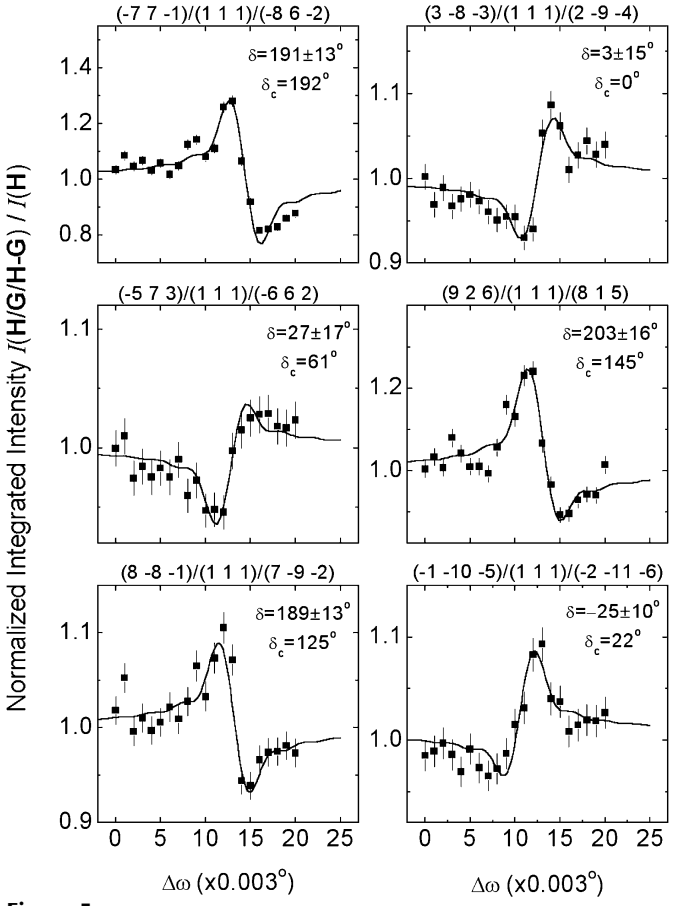

Figure 5
Examples of reference-beam diffraction interference profiles of tetragonal lysozyme measured using the new κ diffractometer. The X-ray wavelength used is $\lambda = 1.1$ Å, and the reference reflection chosen is **G** = (111). The symbols are integrated intensities measured from the RBD oscillation images and the solid curves are analytical fits to the data, yielding the corresponding triplet phases δ. Also shown are the calculated triplet phases δ_c based on Protein Data Bank entry 193L (Vaney *et al.*, 1995).

phase information that we are interested in. By employing a curve-fitting routine based on either a second-order Born approximation (Shen, 1986) or an expanded distorted-wave approach (Shen, 1999*b*, 2000; Shen & Huang, 2001), the triplet phase δ_H can be obtained directly from the measured RBD intensity profiles $I_H(\omega_i)$. Some typical examples of such profiles and curve-fitting results are shown in Fig. 5, obtained on a tetragonal lysozyme crystal at room temperature. The fitting procedure is repeated for all reflections recorded on the CCD, giving rise to a complete set of measured triplet phases that can potentially be used in conjunction with *e.g.* direct methods to solve a protein crystal structure (Weeks *et al.*, 2000).

5. Conclusions

In summary, we have described the design, the geometry calculations and the alignment strategies of a new five-circle κ diffractometer, specifically designed for reference-beam diffraction measurements of triplet phases in protein crystals. The overall experimental setup as well as the complete procedure for an RBD experiment in an oscillating-crystal camera have been developed and tested. It has been demonstrated that, with the new five-circle κ diffractometer, it is now possible to orient the specimen based on an initial oscillation image, to align an arbitrary reference reflection **G** onto the oscillation axis ψ, and to collect a complete RBD triplet-phase data set, all in a reasonable period of time, *e.g.* 12 h, at a synchrotron facility.

With further research and development, it is our hope that the reference-beam diffraction technique could become one of several practical experimental phasing methods in protein crystallography.

We gratefully acknowledge Karl Smolenski and Walt Protas for their help in the design and construction of the κ diffractometer, Marian Szebyeni and Chris Heaton at MacCHESS for technical assistance during the experiments, and Alexsei Kisselev and Ivan Dobrianov in Professor Robert Thorne's group at Cornell for the lysozyme crystals. This work is supported by National Science Foundation Grant DMR 97-13424 through CHESS, and by the National Institutes of Health Grant GM-46733 through the Hauptman-Woodward Medical Research Institute in Buffalo, New York.

References

ADSC (2001). Area Detector System Corporation, 12550 Stowe Drive, Poway, California 92064, USA. (http://www.adsc-xray.com/.)
Busing, W. R. & Levy, H. A. (1967). *Acta Cryst.* **22**, 457–464.
Collaborative Computational Project, Number 4 (1994). *Acta Cryst.* D**50**, 760–763.
Certified Scientific Software (2002). PO Box 390640, Cambridge, MA 02139, USA. (http://www.certif.com/.)
Chang, S. L. (1982). *Phys. Rev. Lett.* **48**, 163–166.
Chang, S. L., Chao, C. H., Huang, Y. S., Jean, Y. C., Sheu, H. S., Liang, F. J., Chien, H. C., Chen, C. K. & Yuan, H. S. (1999). *Acta Cryst.* A**55**, 933–938.
Chao, C. H., Hung, C. Y., Huang, Y. S., Ching, C. H., Lee, Y. R., Jean, Y. C., Lai, S. C., Stetsko, Y. P., Yuan, H. & Chang, S. L. (2002). *Acta Cryst.* A**58**, 33–41.
Colella, R. (1974). *Acta Cryst.* A**30**, 413–423.
Huber (2001). Huber Diffraktionstechnik GmbH. (http://www.xhuber.com/default.htm.)
Shen, Q. (1986). *Acta Cryst.* A**42**, 525–533.
Shen, Q. (1998). *Phys. Rev. Lett.* **80**, 3268–3271.
Shen, Q. (1999*a*). *Phys. Rev. B*, **59**, 11109–11112.
Shen, Q. (1999*b*). *Phys. Rev. Lett.* **83**, 4784–4787.
Shen, Q. (2000). *Phys. Rev. B*, **61**, 8593–8597.
Shen, Q. & Huang, X. R. (2001). *Phys. Rev. B*, **63**, 174102-1–174102-8.
Shen, Q., Kycia, S. & Dobrianov, I. (2000*a*). *Acta Cryst.* A**56**, 264–267.
Shen, Q., Kycia, S. & Dobrianov, I. (2000*b*). *Acta Cryst.* A**56**, 268–279.
Shen, Q., Pringle, D., Szebenyi, M. & Wang, J. (2001). *Rev. Sci. Instrum.* **73**, 1646–1648.
Thorkildsen, G., Mathiesen, R. H. & Larsen, H. B. (1999). *J. Appl. Cryst.* **32**, 943–950.
Vaney, M. C., Maignan, S., Ries-Kautt, M. & Ducruix, A. (1995). Deposited with Protein Data Bank, PDB ID: 193L.
Weckert, E. & Hummer, K. (1997). *Acta Cryst.* A**53**, 108–143.
Weeks, C. M., Xu, H., Hauptman, H. A. & Shen, Q. (2000). *Acta Cryst.* A**56**, 280–283.